Check for updates

ASCE

Uncertainty Quantification in Fault Tree Analysis: Estimating Business Interruption due to Seismic Hazard

Saurabh Prabhu[1]; Carl Ehrett[2]; Mohammad Javanbarg[3]; D. Andrew Brown[4]; Marc Lehmann[5]; and Sez Atamturktur[6]

Abstract: This paper presents an approach based on fault tree analysis and subset simulation for quantifying uncertainty in the risk assessment of complex industrial facilities. Downtime estimation of industrial facilities after an extreme event is critical for risk valuation, as business interruption contributes significantly to monetary losses. Industrial facilities are complex systems with many critical, interdependent components. Such facilities are thus amenable to modeling using fault trees. Fault tree analysis breaks down a facility's layout into system components and links component failure probabilities through Boolean logic to estimate the larger system's failure probability. In estimating system failure probability, the lack of knowledge about failure probabilities of individual components introduces uncertainty. Subset simulation offers an efficient approach for propagating these component-level uncertainties to the system level. However, when parameters are highly correlated, traditional algorithms used in subset simulation may suffer from low acceptance rates (ratio of new samples to total samples), resulting in repeated samples, thereby compromising efficiency. This paper demonstrates that the proposed treatment allows application of subset simulation to uncertainty quantification of large fault trees using a case study of a coal-fired power plant. **DOI: 10.1061/(ASCE)NH.1527-6996.0000360.** *© 2020 American Society of Civil Engineers.*

Author keywords: Risk assessment; Subset simulation; Systems analysis; Business interruption; Restoration; Industrial facility.

Downloaded from ascelibrary.org by Clemson University on 02/26/20. Copyright ASCE. For personal use only; all rights reserved.

Introduction

Following major natural disasters, losses from business interruption represent a significant percentage of total monetary loss and can far exceed losses from property damage, especially in industrialized regions (Tierney 1997; Alesch and Holly 1998; Chang 2000; Alesch et al. 2001; Chang and Falit-Baiamonte 2002; Erdik and Durukal 2003; Kunz et al. 2013; Tatano and Kajitani 2012; Krausmann and Cruz 2013; Barlyn 2017). In seismic risk assessment, methods for estimating property damage have been extensively studied; however, little attention has been given to estimating losses from business interruption (Godschalk 2003; Webb et al. 2000; Heatwole and Rose 2013; Yang et al. 2016). Indeed, no industry standard for downtime estimation currently exists. Although projects such as HAZUS (FEMA 2010) and ATC-25 (ATC 1991) have provided downtimes for generic lifeline facilities based on empirical data and expert opinion, these downtimes do not account for site-specific layout and dependencies between the components and are thus useful only in regional loss assessment context and not in a site-specific context.

Industrial facilities, such as power plants and oil refineries, are systems composed of several interdependent structural, mechanical, and electrical components (Kiremidjian et al. 1985). Such facilities are therefore appropriate for representation using fault trees (Flammini et al. 2005; Lindhe et al. 2009; Norberg et al. 2009; Rao et al. 2009; Porter and Ramer 2012). Fault trees estimate the failure probability of a facility based on the failure probabilities specified for each of the facility's critical components. Values for component-level failure probabilities are defined by (1) *fragility curves* that represent the conditional probability of a component failing (i.e., exceeding a damage state) given a seismic demand parameter [e.g., peak ground acceleration (PGA), spectral acceleration, drift ratio] (Hwang and Chou 1998; Unanwa et al. 2000; Simpson et al. 2005; Huang et al. 2011), and (2) *restoration curves* that represent the probability of a component being repaired in given time for a given damage state (Carpaneto et al. 2005; Liu et al. 2007).

In this paper, both fragility and restoration curves are defined as parametric cumulative distribution functions, with uncertainties existing in their parameters primarily as a result of scarce historical data about component failures. A cumulative distribution is chosen because of the definition of system failure, discussed later. Moreover, as seen in the case-study demonstration, using cumulative distributions allows calculation of downtime for the full spectrum of hazards. However, for point probability estimates, component failure probabilities may be specified for a single event or group of events. Characterizing system-level uncertainty that results from uncertainty at the level of individual components is important for loss estimation and risk valuation. Yet such systemic characterizations present a computationally challenging task because fault tree models of industrial facilities often include a large number (up to 300) of critical components (US Nuclear Regulatory Commission 1983).

[1]Senior Catastrophe Research Analyst, American International Group, 175 Water St., New York, NY 11201. Email: Saurabh.Prabhu@aig.com

[2]Ph.D. Candidate, Dept. of Mathematical Sciences, Clemson Univ., Clemson, SC 29631. Email: cehrett@clemson.edu

[3]Director of Product Development, American International Group, 175 Water St., New York, NY 11201. Email: Mohammad.Javanbarg@aig.com

[4]Assistant Professor, Dept. of Mathematical and Statistical Sciences, Clemson Univ., Clemson, SC 29631. ORCID: https://orcid.org/0000-0003-2715-7190. Email: ab7@clemson.edu

[5]Head, Client CAT Analytics, American International Group, 58 Fenchurch St., London EC3M 4AB, UK. Email: Marc.Lehmann@aig.com

[6]Harry and Arlene Schell Professor and Head of the Department of Architectural Engineering, Pennsylvania State Univ., 104 Engineering Unit A, State College, PA (corresponding author). ORCID: https://orcid.org/0000-0003-3653-1260. Email: sez@psu.edu

Note. This manuscript was submitted on July 18, 2018; approved on August 5, 2019; published online on February 26, 2020. Discussion period open until July 26, 2020; separate discussions must be submitted for individual papers. This paper is part of the ***Natural Hazards Review***, © ASCE, ISSN 1527-6988.

For such high-dimensional reliability problems, subset simulation (Au and Beck 2001; Bect et al. 2017) offers an efficient algorithm, especially for estimating small limit-state probabilities. In subset simulation, the failure probability at a given threshold is expressed as the product of failure probabilities corresponding to a series of larger failure regions. Resampling in the larger failure regions is typically achieved using Markov chain Monte Carlo methods.

This paper proposes a fault tree methodology for estimating downtime of industrial facilities. Such methodology allows one to consider each component of a complex system separately when estimating the downtime. The uncertainty in the model's variables is propagated using subset simulation. An alternative to the sampling algorithms originally used in subset simulation is developed to increase efficiency by leveraging correlations between parameters in the failure region. The motivating application discussed in this paper is determining the downtime estimation for a coal-fired power plant after seismic events.

Background on Fault Tree Approach

Fault Tree Analysis for Business Interruption Estimation

A fault tree is a graphical model that can be used for conducting a reliability analysis of any system consisting of discrete components with independent probabilities of failure (Lapp and Powers 1977; Vesely et al. 1981; Lee et al. 1985; Ruijters and Stoelinga 2015). An advantage of the fault tree approach is its intuitive and graphical modeling of a larger facility or system; by connecting components using logic gates, the fault tree approach allows for a straightforward representation of the dependencies between components and the redundancies within a system. In addition, fault tree analysis permits one easily to make modifications that change the component states or failure probabilities within a system; this modifiability enables both sensitivity analysis to identify critical components and cost–benefit analysis to optimize loss mitigation. Such versatility makes fault tree analysis a suitable approach for reliability assessments of industrial facilities.

In this analysis, each component is assigned a probability of failure propagated via logic gates to obtain the failure probability of a system as a whole. More specifically, AND gates and OR gates combine the failure probabilities of system components based on the layout of the system itself. The combined failure probability $P(C)$ of subsystem C, which is composed of components $[c_1, \ldots, c_{n_c}]$ that are connected with AND and OR gates, is calculated as

$$P(C|AND) = \prod_{i=1}^{n_c} P(c_i) \tag{1}$$

$$P(C|OR) = 1 - \prod_{i=1}^{n_c} (1 - P(c_i)) \tag{2}$$

where $P(c_i)$ is the failure probability of the ith component connected to the gate. Components connected by an OR gate represent a "weakest link" or serial system in which the failure of any component results in system failure. Meanwhile, components connected by an AND gate represent a "parallel" system in which all components must fail for the system to fail. Although AND and OR gates are most commonly applied in engineering risk assessment problems, several other gates (e.g., priority gates and delay gates) adding specialized functionality can be applied (Roberts et al. 1981).

To estimate downtime, this study assumes binary component states: functional or nonfunctional (Porter and Ramer 2012). The probability that a component is nonfunctional is determined based on (1) the probability of that component, subject to demand parameter s, being *damaged*, and (2) the probability of that component being *unrepaired* before time t. The probability that the ith component will be damaged is obtained from fragility curve $H(s)$, while the probability that the damaged component will be repaired is obtained from restoration curve $G(t)$. Thus, $(1 - G(t))$ gives the probability that the component will be unrepaired. In a system with n_c components, the probability of component i being in a nonfunctional state at time t subject to demand parameter s is then given as follows:

$$P^{(i)}(s,t) = H^{(i)}(s)(1 - G^{(i)}(t)); \quad i = 1, \ldots, n_c \tag{3}$$

In Eq. (3), the fragility and restoration curves are considered statistically independent in that the probability of a repair time exceeding t is defined independently of the probability of damage under demand parameter s. However, the fragility and restoration curves can be dependent on damage states as given in the following equation:

$$P^{(i)}(s,t) = 1 - \prod_{d=1}^{n_d} (1 - H_d^{(i)}(s)(1 - G_d^{(i)}(t))); \quad i = 1, \ldots, n_c \tag{4}$$

Damage states classify the incremental levels of damage to a structure (e.g., slight, moderate, or extensive). Thus, while the functionality of a component is binary (i.e., functional or nonfunctional), the damage to a component can assume multiple states. The fragility $H_d(s)$ for a given damage state acts as a weighting factor for the restoration function in Eq. (4).

In this study, the partial functionality of a system is not considered for explanatory purposes. It is, however, trivial to consider partial functionality by adding repair states corresponding to the partial functionality of components, i.e., providing restoration curves for, say, 50% capacity. Since partial functionality is not considered here, a system or facility is assumed to be in a nonfunctional state until all subsystems are brought to a fully functional state. Thus, only the components critical to system operation are included in the fault tree model, and the probability of system failure, $F_{\text{top}}(s,t)$, is calculated using Eqs. (1) and (2). Using these two equations allows combining the individual failure probabilities of components based on the system layout of the larger facility. The system failure probability is defined as *the system being non-functional for time less than t, given a site excitation of magnitude s*. Note that this definition of system failure requires the use of cumulative distributions for both fragility and restoration curves. In the absence of such information, the system failure definition may be changed without altering the general methodology. After evaluating the fault tree for a range of values for t and s, the cumulative distribution $F_{\text{top}}(t,s)$ of the system failure probability is then calculated as the probability that the downtime is less than t for excitation magnitude s. From this distribution, the mean downtime $E(t|s)$ of the system for a given excitation magnitude s is obtained using the following equations:

$$f(t|s) = \frac{d(F_{\text{top}}(t,s))}{dt} \tag{5}$$

$$E(t|s) = \int_0^\infty t \cdot f(t|s)dt \tag{6}$$

where $f(t|s)$ is the probability density function associated with the probability that a component is nonfunctional for time t given site

Downloaded from ascelibrary.org by Clemson University on 02/26/20. Copyright ASCE. For personal use only; all rights reserved.

excitation s. $f(t|s)$ is obtained by taking the first derivative of $F_{\text{top}}(t, s)$ with respect to time t.

Fragility Modeling

Fragility curves provide the component failure probability, $H(s)$, for the fault tree analysis. Within seismic analysis, the fragility curve of a component reflects the probability of the component being in or exceeding a certain damage state as a function of the intensity measure. Fragility curves are functions of intensity of seismic demand parameters, such as PGA, spectral acceleration, or interstory drift. Fragility curves are developed using either a data-based (Sabetta et al. 1998; Basoz et al. 1999; Colombi et al. 2008; Lantada et al. 2010) or a model-based approach (Singhal and Kiremidjian 1996; Shinozuka et al. 2000; Ellingwood 2001; Gardoni et al. 2003). The data-based approach relies on post-disaster site evaluations to aggregate historical data related to a system component's seismic damage; in contrast, the model-based approach involves developing physics-based numerical models of system components, simulating a range of seismic forces using nonlinear dynamic analysis to compute seismic response (Singhal and Kiremidjian 1996; Ibarra and Krawinkler 2005; Rossetto and Elnashai 2005; Hamburger et al. 2012). The advantage of a data-based approach is that one relies on true observations rather than the approximations made in a model-based approach. On the other hand, postdisaster data are hard to come by, while model simulations can be performed over a wide range of disaster scenarios. Detailed information on fragility curve development and usage is found in Der Kiureghian (1996), Shome (1999), Shinozuka et al. (2000), and Pinto et al. (2004).

Typically, fragility curves are represented by a two-parameter lognormal cumulative distribution function (Pagni and Lowes 2006; Bradley and Dhakal 2008; Lallemant et al. 2015). The fragility curve for damage state d is then given as

$$H_d(s) = \mathcal{F}\left[\frac{\ln\left(\frac{s}{\mu_{d,s}}\right)}{\sigma_{d,s}}\right]; \quad d = 1, \ldots, n_d \tag{7}$$

The values for the mean μ and standard deviation σ are determined by curve fitting to empirical or analytical data (Lallemant et al. 2015; Noh et al. 2015). The advantages of using a lognormal cumulative distribution function for this application are twofold. First, the abscissa has a lower bound of 0, which is convenient because seismic demand parameters are typically positive values. Second, multiplication or division of the distribution parameters by a factor of safety preserves the parameters' lognormal nature.

The fragility curve typically captures the aleatory uncertainty in predicting a system's response (Hamburger et al. 2004; Kircher et al. 2006). Epistemic uncertainty may also be considered by artificially adding variance to the distribution function based on the analyst's judgment. Outside of regions that have advanced seismic detection infrastructure (e.g., California and Japan), ground motion prediction equations are used to estimate a demand parameter, such as the ground-shaking intensity at the site of a facility (Lallemant et al. 2015). Specific to the regions where empirical data are collected, such equations are developed based on earthquake magnitude, distance of the site from the seismic source, and site characteristics, such as soil type. Both intraevent (within each event) and interevent (between events) uncertainties affect the development of these equations (Gregor et al. 2014). Typically, several equations relevant to a site of seismic activity are weighted according to expert opinion and then combined; this strategy of handling equations adds yet another source of uncertainty to fragility modeling. Meanwhile, additional complications arise depending on whether ground motion

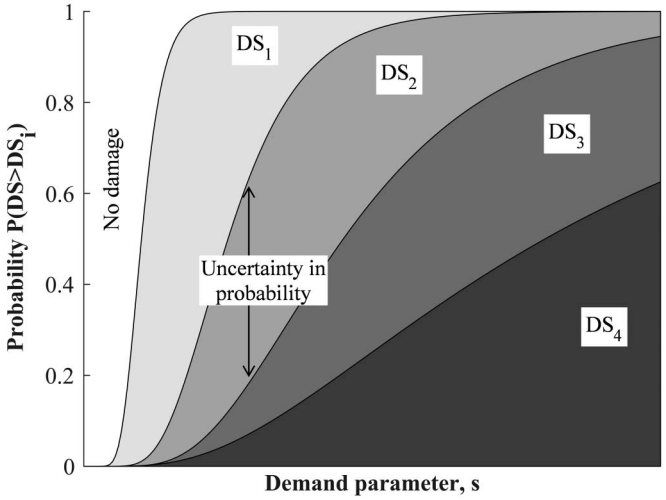

Fig. 1. Representative fragility curves for Damage States DS1–DS4.

is considered variable or uniform. Several studies have found that accounting for spatial variation in ground motion leads to a significantly larger probability of damage than that derived using a spatially uniform ground motion (Lopez et al. 2000; Kim and Feng 2003; Lupoi et al. 2005; Lou and Zerva 2005; Zhang et al. 2009). Therefore, when fragility curves are derived without considering spatial variation in ground motion, their parameter values must be considered uncertain.

Another limitation of fragility curves is that they are often developed for discrete damage states ranging from minor damage to complete collapse (see Fig. 1 showing the uncertainty in estimating the probability of exceeding four discrete damage states). The HAZUS (FEMA 2010; Kircher et al. 2006) earthquake loss estimation methodology, for instance, is based on four damage states: slight (DS_1), moderate (DS_2), extensive (DS_3), and complete (DS_4). Because each of these damage states lacks a standardized, objective definition, reliance on such terms heightens the uncertainty associated with applying these fragility curves (Porter 2015). Furthermore, when the fragility curve for a system component is not readily available, it is common practice to use available curves that most closely resemble the component or category of interest. For example, a fragility curve developed for rotating machinery may be used for a diesel generator in the absence of data for the latter. Such generalizations and substitutions ultimately add to uncertainty in the fragility curves.

Because fragility analysis is subject to multiple sources of uncertainty, it is imperative to consider those sources when specifying probability distributions on the parameters. Typically, fragility curves take the form of lognormal cumulative distribution function with two parameters, the median and log standard deviation. In this study, the two parameters are assigned uniform distributions with intervals based on judgment from the authors' field experience. Using uniform distributions on unknown parameters is also common in the computer experiment literature (Williams et al. 2006; Higdon et al. 2008; Brown and Atamturktur 2018).

Restoration Modeling

For fault tree analysis, restoration curves provide the probability of a component being restored to full functionality after a disaster event, $G_d(t)$. Similar to fragility curves, restoration curves can be obtained through either a data-based or a model-based method. Data-based methods (i.e., empirical restoration curves) do not

Downloaded from ascelibrary.org by Clemson University on 02/26/20. Copyright ASCE. For personal use only; all rights reserved.

reflect the actual restoration process; instead, they relate hazard intensity to facility downtime. In what may be considered the simplest data-based method, the restoration curve of a facility can be obtained by fitting a curve to the facility downtime data obtained from similar facilities that have previously experienced earthquakes (Chang et al. 1996; Shinozuka et al. 1998; Comerio 2006; Liu et al. 2007; Nateghi et al. 2011). Typically, data related to facility restoration times are scarce; in consequence, expert opinion regarding repair times is needed to complement the fitted regression models, as was the case with the restoration curves (i.e., ATC-13 and ATC-25) developed by Chang et al. (1996). Because empirical restoration curves are usually generated for generic facility types (e.g., power plants, water supply systems), they seldom account for the specific characteristics of a facility, including its geographic location, its age, and the layout of its components.

Unlike the data-based approach, the model-based approach represents the restoration process using simplified equations and rules that estimate repair time as a function of specific variables, including, but not limited to, the number of available repair personnel, the repair speed, and the priority of the repair (Isumi et al. 1985; Kozin and Zhou 1990; Zhang 1992; Logothetis and Trivedi 1997; Chang and Falit-Baiamonte 2002). The parameters of model-based equations are often derived empirically from historical data or from time-based simulations of the restoration process.

As was the case with fragility curves, restoration curves are often represented as two-parameter lognormal cumulative distribution functions for varying damage states:

$$G_d(t) = \mathcal{F}\left[\frac{\ln\left(\frac{t}{\mu_{d,t}}\right)}{\sigma_{d,t}}\right]; \quad d = 1, \ldots, n_d \tag{8}$$

The parameters $\mu_{d,t}$ and $\sigma_{d,t}$ are the mean and standard deviations, respectively, that account for the uncertainty in repair time. Other distribution functions (e.g., normal, Weibull, logistic, and exponential) can also be used to represent restoration curves (Carpaneto et al. 2005; Liu et al. 2007).

Uncertainty in restoration curves primarily stems from the limited historical data available for specific system components. When sufficient historical data are entirely unavailable, restoration times for system components are often informed by subjective expert opinion, as is the case with the ATC-13 restoration curve. However, even when some historical data are available, uncertainty often arises because those data are widely dispersed for reasons including, but not limited to, variability in anchorage conditions, variability in component weights, variability in damage states, and regional variations in repair times. As regards regional variations in repair times, for instance, a heavily damaged steam turbine can be repaired faster if the machine parts do not have to be imported from another country. Thus, in a probabilistic treatment of restoration curves using a lognormal or normal distribution, the distribution parameters must be treated as uncertain. Similar to fragility curves, the two parameters of lognormal distribution are assigned a uniform distribution with intervals based on expert judgment.

Probabilistic Approaches to Uncertainty Quantification in Fault Trees

The means and standard deviations of fragility curves capture variability in factors that are specific to a facility and its site, such as ground motion, structural parameters, and soil conditions. Meanwhile, the means and standard deviations of restoration curves capture variabilities in repair times. However, these parameters must themselves be treated as uncertain quantities when extrapolating to other structures and conditions (Tate et al. 2015). Thus, there are two levels of uncertainty when estimating a system's downtime: the first level is represented by the empirical fragility and restoration curves gathered from historical data, while the second level is represented by the uncertainties in the mean and standard deviation values themselves.

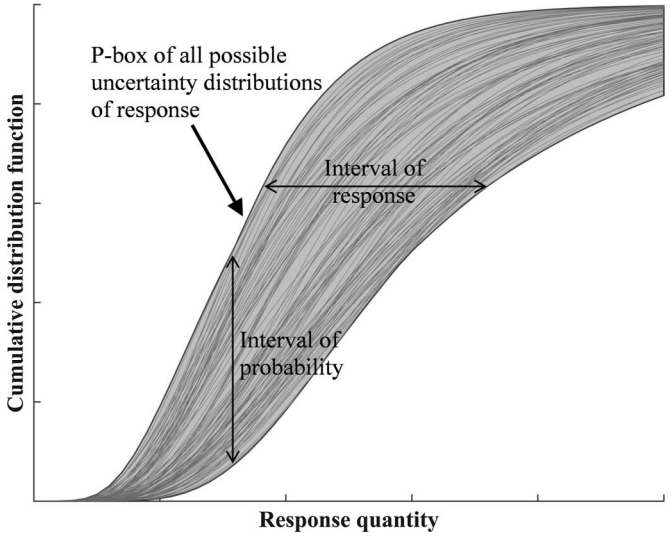

Fig. 2. Example of P-box representation of uncertainty.

In relation to fault tree models, three separate approaches to uncertainty quantification are studied here: the Monte-Carlo simulation, standard subset simulation, and a subset simulation with multivariate resampling. The implementation, advantages, disadvantages, and computational efficiency of each approach are discussed in what follows. That discussion is followed in the next section by an application of the three models to a case study.

Monte Carlo Simulation

The traditional approach to quantifying uncertainties involves separately propagating the two levels of uncertainty mentioned previously using a double-looped Monte Carlo simulation. The parameters representing the uncertainty distribution of each of the n variables are also considered uncertain. With this approach, N_2 samples of each variable's distribution parameters are first drawn to represent the second level of uncertainty. Next, N_1 samples of each variable are drawn from the distributions given by each of the N_2 samples, thereby forming an ensemble of $N = N_1 \times N_2$ samples. The result of this approach is an ensemble of distributions that forms what is known as a probability box, or *P-box* (Karanki et al. 2009). The P-box represents the output quantity as an interval-valued probability (Fig. 2). Thus, the probability of exceeding a given response quantity is no longer a single value but an interval; in similar fashion, the response quantity that can be exceeded with a given probability is represented by an interval. When a double-looped Monte Carlo simulation is applied to fault tree analysis, the simulation may be less than desirable when quantifying uncertainties that involve a large number of input parameters since sparse sampling can result in misleading results (Hemez and Atamturktur 2011).

Consider the following reliability problem:

$$p_F = P(\boldsymbol{\theta} \in F) \tag{9}$$

$$F = \{\boldsymbol{\theta}: g(\boldsymbol{\theta}) < g^*\} \tag{10}$$

Downloaded from ascelibrary.org by Clemson University on 02/26/20. Copyright ASCE. For personal use only; all rights reserved.

Here, p_F is the probability that the performance function $g(\boldsymbol{\theta})$ is less than a threshold g^* in the n-dimensional parameter space $\Theta \subset \Re^n$. The parameters $\boldsymbol{\theta} = (\theta_1, \ldots, \theta_n)$ are uncertain and thus treated as random variables with associated probability distributions. To accurately estimate high-consequence, low-probability events using a Monte Carlo simulation, the number of samples required is proportional to $1/p_F$. For example, if $p_F = 10^{-5}$, one would expect to draw at least $100 \times 10^5 = 10^7$ samples in order to generate approximately 100 samples in F. This large number of samples makes Monte Carlo simulations undesirable for estimating the probabilities of rare events, especially if the function $g(\boldsymbol{\theta})$ is computationally demanding.

The coefficient of variation of the Monte Carlo estimate $\hat{p}_F$ of failure probability p_F is a function of the target probability of failure and the number of samples:

$$cov(\hat{p}_F) = \sqrt{\frac{1 - p_F}{N p_F}} \tag{11}$$

$$\hat{p}_F = \frac{1}{N} \sum_{j=1}^{N} I_F(\boldsymbol{\theta}^{(j)}) \tag{12}$$

Thus, the number of samples required becomes inordinately large to keep the coefficient of variation reasonably small for a small target probability. In the next section, a more efficient method to estimate low-probability events will be discussed.

Subset Simulation

Subset simulation is a Markov chain Monte Carlo–based sampling technique for efficiently drawing samples from low-probability failure regions while being insensitive to the number of uncertain parameters (Caflisch 1998), thus efficiently estimating probabilities of rare events. Subset simulation was introduced by Au and Beck (2001) as a version of the Metropolis–Hastings algorithm (Metropolis et al. 1953; Hastings 1970) that uses the one-dimensional conditional distributions of each of the parameters. In subset simulation, the target failure region associated with a small target probability of failure (rare event) is located through a decreasing sequence *of intermediate* failure regions. The probability of failure is then calculated as the product of a *series of the conditional probabilities of failure* corresponding to the series of larger failure regions:

$$p_F = P(F) = P(F_1) \prod_{k=2}^{m} P(F_k | F_{k-1}) \tag{13}$$

where $F = F_m \subset F_{m-1} \subset \ldots F_2 \subset F_1$ is a sequence of nested failure regions defined by corresponding threshold values $(g_m^*, g_{m-1}^*, \ldots, g_2^*, g_1^*)$. The conditional probability is approximated as

$$P(F_k|F_{k-1}) = P(\boldsymbol{\theta}^{(k)} \in F_k | \boldsymbol{\theta}^{(k)} \in F_{k-1}) = P(g(\boldsymbol{\theta}^{(k)}) < g_k^* | g(\boldsymbol{\theta}^{(k)}) < g_{k-1}^*) \approx \frac{1}{N} \sum_j I_{F_k}(\boldsymbol{\theta}_j^{(k)}) \tag{14}$$

Here, each $\boldsymbol{\theta}_j^{(k)}$ is a realization from the conditional distribution $p(\cdot\,|F_{k-1})$ obtained using the modified Metropolis algorithm (MMA) described in what follows.

At each stage of the MMA, a Markov chain is initialized at $\boldsymbol{\theta}^{(k)} \sim p(\cdot\,|F_{k-1})$. For each parameter θ_l, $l = 1, \ldots, n$, a proposed state ϕ_l is drawn from a proposal distribution $q_l(\cdot\,|\theta_l)$, as would be used in the ordinary Metropolis algorithm. Each element of the candidate state θ_l^* is set to ϕ_l with the acceptance probability given below; otherwise, $\theta_l^* = \theta_l$. To maintain ergodicity (i.e., the guarantee that the correct distribution is sampled), it is required that the support of the proposal distribution completely contain the next failure region F_k (Robert and Casella 2013). [See Au and Beck (2001) for a more detailed discussion of how to ensure F_k is covered.] The candidate state $\boldsymbol{\theta}^* = (\theta_1^*, \ldots, \theta_n^*)$ is accepted as a draw from $p(\cdot\,|F_k)$ if it lies in the next failure region F_k (in which case $\boldsymbol{\theta}^{(k+1)} = \boldsymbol{\theta}^*$), and rejected otherwise.

Suppose that the joint distribution of the parameter vector (without being restricted to any failure region) satisfies $p(\boldsymbol{\theta}) = \Pi_{l=1}^{n} \pi_l(\theta_l)$; i.e., that the parameters are mutually independent a priori. Then the MMA algorithm of Au and Beck (2001) is as follows:

Modified Metropolis Algorithm (Au and Beck 2001)

Initialize
- $k = 1$
- Generate N samples of $\boldsymbol{\theta}^{(1)}$ from the known parameter distribution
- Set $\hat{P}(F_1) = \frac{1}{N} \sum_{i=1}^{N} I_{F_1}(\boldsymbol{\theta}_i^{(1)})$
- Set g_1^* as the $N/10^{th}$ value in $\{g_{(1)}(\boldsymbol{\theta}^{(1)}), \ldots, g_{(N)}(\boldsymbol{\theta}^{(1)})\}$ arranged in descending order, so that $P(F_2|F_1) = 0.1$, where $F_2 = \{\boldsymbol{\theta}: g(\boldsymbol{\theta}) < g_1^*\}$.

for $k = 2, \ldots$
- **for** $j = 1, \ldots, N_s$

  # Generate a candidate state $\boldsymbol{\theta}^*$:
  - **for** $l = 1, \ldots, n$

    # Step 1: Random walk
    - Draw ϕ_l from the proposal distribution $q_l(\cdot\,|\theta_l^{(k)})$
    - Set $\theta_l^* = \phi_l$ with the probability $\min\left(1, \frac{\pi_l(\phi_l)}{\pi_l(\theta_l^{(k)})}\right)$

    end for

    # Step 2: Check whether candidate is in the next failure region
  - Check if $\boldsymbol{\theta}^* \in F_k$

    $\boldsymbol{\theta}_j^{(k)} = \begin{cases} \boldsymbol{\theta}^* & \text{if } \boldsymbol{\theta}^* \in F_k \\ \boldsymbol{\theta}_j^{(k-1)} & \text{if } \boldsymbol{\theta}^* \notin F_k \end{cases}$

    Set $j \leftarrow j + 1$

end for
- Set g_k^* as the $N/10^{th}$ value $\{g_{(1)}(\boldsymbol{\theta}^{(k)}), \ldots, g_{(N)}(\boldsymbol{\theta}^{(k)})\}$ arranged in descending order
- **if** $g_k^* < g_{target}^*$
  - $m = k$
  - **break for**

end for
- $\widehat{p_F} = \hat{P}(g(\boldsymbol{\theta}) < g_{target}^*) = \hat{P}(F_1) \prod_{k=2}^{m} \hat{P}(F_k|F_{k-1}) = \hat{P}(F_1) * 0.1^m$

The choice of a constant $\hat{P}(F_k|F_{k-1}) = 0.1$ is based on the suggestion by Au and Beck (2001). Zuev et al. (2012) show that the target distribution $p(\cdot\,|F = F_m)$ is, in fact, the stationary distribution of the Markov chain.

Subset Simulation with Multivariate Draw

The modified Metropolis algorithm described in Au and Beck (2001) is most efficient when the parameters are independent with respect to the failure region, i.e., if $I_F(\boldsymbol{\theta}) = \Pi_l I_{F_l}(\theta_l)$ for some collection of sets $F_1, \ldots, F_n$. However, a failure region that induces dependence among the parameters can lead to an undesirably low probability that a candidate sample $\boldsymbol{\theta}^*$ will be accepted. For instance, if $F = \{\boldsymbol{\theta} = (\theta_1, \theta_2): \theta_1^2 + 1.75\theta_1\theta_2 + \theta_2^2 < 1\}$, then $F \neq F_1 \times F_2$ for any choice of F_1, F_2. In this case the parameters will be

Downloaded from ascelibrary.org by Clemson University on 02/26/20. Copyright ASCE. For personal use only; all rights reserved.

dependent with respect to the failure region F, and sampling θ_1 and θ_2 from their marginal distributions separately can lead to a higher probability of rejection. To mitigate this situation, an adaptive multivariate proposal distribution is used with a covariance matrix that is estimated from the correlation among the sampled parameters (Haario et al. 2001; Carlin and Louis 2009) lying in each intermediate failure region. The difference between the modified Metropolis algorithm of Au and Beck (2001) and using a multivariate draw lies in the proposal distribution. Instead of iterative single-site updating for all parameters, a multivariate proposal distribution leverages the covariance between the parameters in the failure region to obtain proposal densities that more closely concentrate on the intermediate failure regions and, thus, is more likely to propose a state that lies in each failure region and will be accepted. Making use of this covariance between parameters improves the acceptance rate of the parameters in Step 2 of the MMA algorithm. Indeed, such multivariate proposals for blocks of correlated parameters are known to improve the performance of more general Markov chain Monte Carlo algorithms (Liu et al. 1994).

In the multivariate draw algorithm, a candidate $\boldsymbol{\theta}^*$ is generated by a single draw from a multivariate normal proposal distribution. If the model parameters have distributions with bounded support, it is helpful to eliminate the boundaries before using a normal proposal distribution. This is accomplished first by rescaling each θ_l so that $\boldsymbol{\theta}$ lies in the unit hypercube followed by using the logit transform $\eta_l := \log(\theta_l/(1-\theta_l))$; $l = 1, \ldots, n$. A multivariate normal distribution is determined by its mean and covariance matrix. On each step of the proposed algorithm, the mean is taken to be the current state of the Markov chain. To estimate the covariance matrix $\boldsymbol{\Sigma}_1$ for this proposal distribution, first, N samples are generated from the target (uniform) distribution of the parameter $\boldsymbol{\theta}$. Next, the sample covariance $\mathbf{S}_1$ is found for the samples that fall into the first intermediate failure region, F_1, that corresponds to the threshold g_1^*. When there is a strong correlation among parameters, the sample covariance matrix $\mathbf{S}_1$ may be almost singular, which makes matrix inversions computationally unstable. Computational stability can be improved by taking $\boldsymbol{\Sigma}_1 := \mathbf{S}_1 + \iota\mathbf{I}$, where ι is a small constant (a "nugget") (Ababou et al. 1994) and $\mathbf{I}$ is the identity matrix. At each iteration k of the subset simulation, N new samples are drawn using covariance matrix $\boldsymbol{\Sigma}_k$. The covariance matrix is updated at every level k of the subset simulation. If the target failure region has not yet been reached, then a new intermediate threshold g_{k+1}^* and corresponding intermediate failure region are defined using the most recent samples, which are then used to construct a new covariance matrix $\boldsymbol{\Sigma}_{k+1}$.

The multivariate draw algorithm differs in principle from the MMA only in the step where a candidate is generated. The algorithm is given below:

Multivariate Draw Algorithm

Initialize
- $k = 1$
- Generate N samples of $\boldsymbol{\theta}^{(1)}$ from the known parameter distribution
- $\hat{P}(F_1) = \frac{1}{N}\sum_{i=1}^{N} I_{F_1}(\boldsymbol{\theta}_i^{(1)})$
- Set g_1^* as the $N/10^{th}$ value $\{g_{(1)}(\boldsymbol{\theta}^{(1)}), \ldots, g_{(N)}(\boldsymbol{\theta}^{(1)})\}$ arranged in descending order, thus $\hat{P}(F_2|F_1) = 0.1$
- **for** $k = 2, \ldots$
  - Find the covariance matrix $\boldsymbol{\Sigma}_\mathbf{k} = \widehat{Var}\{\boldsymbol{\theta}^{(k-1)}\}$. If $\boldsymbol{\Sigma}_\mathbf{k}$ is singular or almost singular, add a nugget to improve computational stability.
  - **for** $j = 1, \ldots, N_s$
    # Generate a candidate state $\boldsymbol{\theta}^*$:
    # Step 1: Multivariate draw
    - Draw $\boldsymbol{\theta}^*$ from the multivariate Normal proposal distribution $q(\cdot\,|\boldsymbol{\eta}^{(k)}, \boldsymbol{\Sigma}_\boldsymbol{k})$, where $\boldsymbol{\eta}^{(k)} = (\eta_1^{(k)}, \ldots \eta_n^{(k)})$ is defined by the logit transformation above.

    Step 2: Check whether candidate is in failure region
    - Check if $\boldsymbol{\theta}^* \in F_k$

    $$\boldsymbol{\theta}_j^{(k)} = \begin{cases} \boldsymbol{\theta}^* & \text{if } \boldsymbol{\theta}^* \in F_k \\ \boldsymbol{\theta}_j^{(k-1)} & \text{if } \boldsymbol{\theta}^* \notin F_k \end{cases}$$

  end for
  - Set g_k^* as the $N/10^{th}$ value $\{g_{(1)}(\boldsymbol{\theta}^{(k)}), \ldots, g_{(N)}(\boldsymbol{\theta}^{(k)})\}$ arranged in descending order
  - **if** $g_k^* < g_{\text{target}}^*$
    - $m = k$
    - **break for**

  end for
- $\widehat{p_F} = \hat{P}(g(\boldsymbol{\theta}) < g_{\text{target}}^*) = \hat{P}(F_1)\prod_{k=2}^{m}\hat{P}(F_k|F_{k-1}) = \hat{P}(F_1) * 0.1^m$

Note that other advances to subset simulation have been made since the seminal work of Au and Beck (2001), some of which address the low acceptance rates that can occur with irregular failure regions. For instance, Zuev and Katafygiotis (2011) combine the original subset simulation algorithm with the so-called delayed rejection algorithm of Tierney and Mira (1999). Their approach is to test whether a candidate $\boldsymbol{\theta}^*$ is in the failure region and, if not, update only those elements of $\boldsymbol{\theta}^*$ that were left unchanged by the previous scan of elementwise Metropolis updates, modifying the acceptance probabilities to preserve ergodicity. In doing so, they propose a new state that is "close" to the first proposal $\boldsymbol{\theta}^*$ with the hopes of accepting the new realization. Such an approach can inflate the number of times the performance function needs to be evaluated (since one might have to evaluate it at least twice to produce one accepted state), which is undesirable when the performance function is computationally expensive. By contrast, the approach used here jointly proposes a new $\boldsymbol{\theta}^*$ that is virtually guaranteed to differ from the current $\boldsymbol{\theta}$ in every element. The multivariate draw approach evaluates the performance function only once before moving on to consider an entirely new state. The multivariate draw approach proved to be convenient for the fault tree analysis considered here. In the sequel, this approach is briefly compared to the original subset simulation algorithm. However, a more exhaustive comparison to more recent modifications and the concomitant analyses are beyond the scope of this paper. Such investigation will be conducted in future work.

Case-Study Demonstration

Power plants present a suitable case study for demonstrating the methodologies discussed in the previous two sections due to the complex system layout and the high potential for business interruption losses following hazardous events, which can exceed property damage losses. In this section, a fault tree model of a coal-fired power plant is developed to estimate the downtime of the plant after seismic events of various magnitudes. Although the facility's name and location are undisclosed, the application of presented methodologies can be demonstrated regardless.

Development of Fault Tree Model

A typical coal-fired power plant consists of eight major subsystems: a conveyance system, a boiler, an air recirculation system, a flue

Downloaded from ascelibrary.org by Clemson University on 02/26/20. Copyright ASCE. For personal use only; all rights reserved.

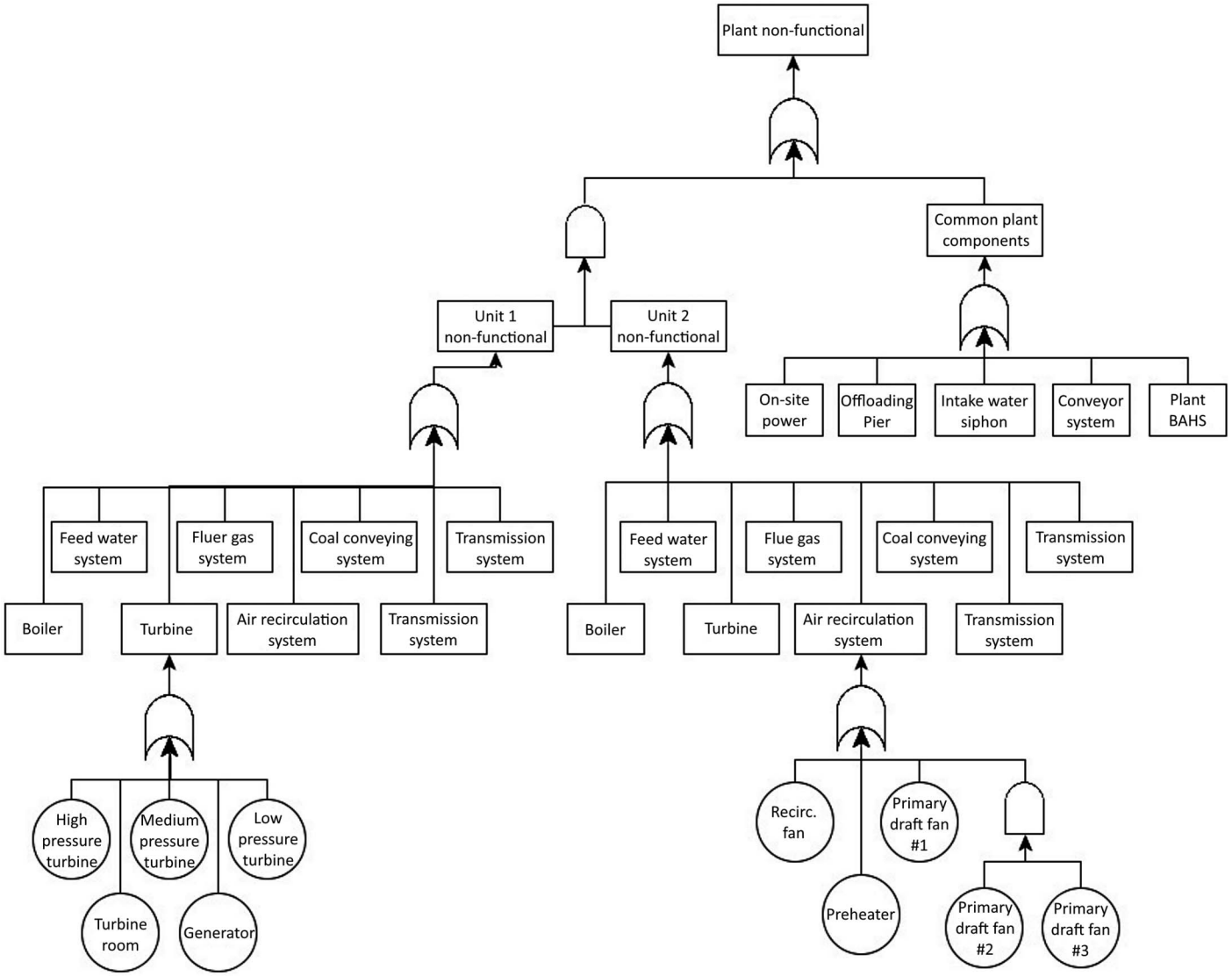

Fig. 3. Fault tree model of coal-fired power plant with two generation units. Some subsystems have been expanded to reveal the constituent components.

gas system, a feed water system, a generation system, a cooling system, and a transmission system. Fig. 3 shows the fault tree of a representative coal-fired power plant. As the figure indicates, a majority of the system components are essential and are therefore connected by OR gates in the fault tree model. Meanwhile, redundancies in the system (e.g., auxiliary silos, tanks, pumps, and transformers) are connected by AND gates. The failure probability of each subsystem is calculated using Eqs. (1) and (2) depending on whether the components in the subsystem are in an AND or OR configuration. Subsequently, the failure probability of the total system is calculated based on the configuration of the subsystems. Subsystems may be nested, i.e., one subsystem can contain multiple subsystems connected in AND or OR configurations. The input hazard is the local PGA of the earthquake. Each component's failure probability corresponding to a given PGA and downtime is estimated using Eq. (4). After generating the failure probability for a range of PGA values and downtime values, the mean downtime is estimated using Eqs. (5) and (6).

The vast majority of empirical fragility curves for grounded equipment are derived in terms of PGA. Furthermore, generally acceptable formulas for approximating PGA from felt earthquake magnitudes (Modified Mercalli Intensity) are readily available in the pertinent literature (Wald et al. 1999). Moreover, since most equipment at the power plant is ground-based, PGA is a suitable intensity measure.

Model Verification

The power plant's mean downtime, obtained from the process described in the background section of the paper, is compared with the downtime curves provided by HAZUS-MH (FEMA 2010) and ATC-25 (ATC 1991) for medium-sized power plants. HAZUS-MH categorizes damage at power generation facilities as medium damage, extensive damage, or complete damage and provides the facilities' downtimes (HAZUS-MH MR5 Table 8.22) as functions of site PGA. These three damage states are combined to estimate failure probability based on Eq. (4).

ATC-25 was developed in 1991 for the purpose of assessing the seismic vulnerability of lifeline systems based on the opinion of a technical advisory group consisting of experts in earthquake engineering. Although industrial design has come a long way in the last three decades, ATC-25 damage and restoration functions are still

Downloaded from ascelibrary.org by Clemson University on 02/26/20. Copyright ASCE. For personal use only; all rights reserved.

Table 1. Peak ground acceleration during and corresponding downtimes after recorded earthquakes at power plant

Earthquake	Magnitude	Peak ground acceleration (g)	Downtime (days)
1965 La Ligua	M7.4	0.27	32
1971 Valparaiso	M7.5	0.16	23
2010 Maule	M8.8	0.2	11

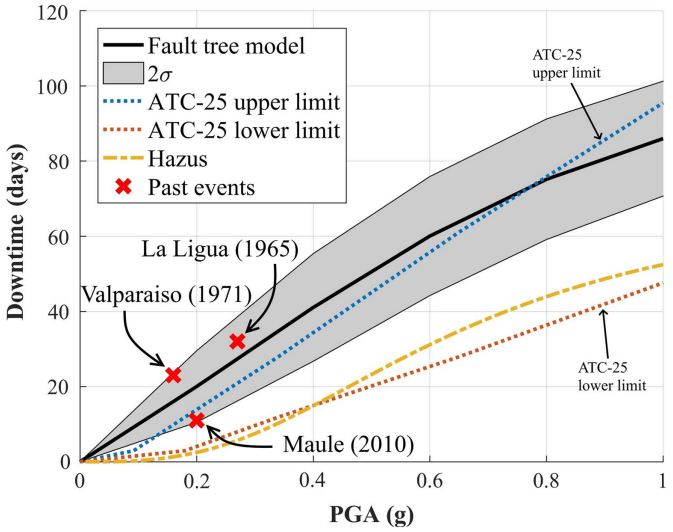

Fig. 4. Fault tree model predictions of downtime for case-study power plant compared with ATC-25 and HAZUS predictions.

widely used for risk analysis, primarily because no follow-up or later study on such a magnitude has been undertaken since that time. ATC-25 provides the downtime of power plants as a function of the Modified Mercalli Intensity, which is converted to PGA using relations from Wald et al. (1999) for comparison. This conversion produces an upper and lower estimate of PGA values corresponding to Modified Mercalli Intensity values, thus generating two downtime curves. Downtimes (from ATC-25 Fig. B-45) are inferred based on the assumption that a power plant is functional only when 100% restoration of capacity is achieved.

For validation, three past events at the case-study power plant and their respective downtimes are available (EPRI 2007). The events and their corresponding PGA values and downtimes are reported in Table 1. As seen in Fig. 4, the three events lie within the 2σ bounds obtained from uncertainty analysis considering the uncertainty in the model parameters discussed in the next subsection. Fig. 4 also compares the downtimes obtained from the fault tree analysis of the power plant to the estimates provided by HAZUS and ATC-25 for generic fossil fuel power plants. The gray band in Fig. 4 shows 2σ obtianed by uncertainty analysis using Monte Carlo simulation. Data in the figure make it clear that, compared to HAZUS, the fault tree model provides almost 60% higher downtime estimates. Although both HAZUS estimates and the lower limit of the ATC-25 estimates fail to capture the past events at the power plant, the upper limit of the ATC-25 estimates does show a closer agreement with the mean prediction of the fault tree model.

The discrepancy between the fault tree model and the empirical curves of HAZUS and ATC-25 can be attributed to the fact that unique features of the power plant are not incorporated in the empirical curves. For instance, the coal offloading pier at the case-study power plant accounts for the highest contribution to the plant's downtime, yet most power plants included in the empirical databases do not have an offloading pier, which results in an underestimation of downtime. In addition, the empirical relations do not incorporate the component repair times that are dependent on geography, availability of labor, or infrastructure, for example. Each of these factors is best known only by plant management. For example, total damage to the boiler could require ordering new machinery, a situation taking anywhere from a few days to several months depending on the plant's location with respect to the distributor. As opposed to empirical curves, fault tree analysis allows for directly taking into consideration both management's insight into repair times and the extent of damage following an earthquake.

Characterizing Component Uncertainties

The fragility and restoration curves developed for this research give the probability that each component of the fault tree will be in a nonfunctional state. Three damage states are consider for each system component of the case-study power plant: low, medium, and high. The failure probability of each component is therefore defined by three fragility curves and three restoration curves corresponding to the three damage states. Both the fragility and the restoration curves are defined by two parameters: the mean and the standard deviation. The categorization of damage states and the selection of parameters for the plant components result in a total of 12 parameters for each component (3 damage states $\times$ 2 parameters of lognormal function for both fragility and restoration curves = 12 parameters), or 1,416 parameters for the 118 system components. Although the component failure probabilities are combined using simple arithmetic at the fault tree logic gates, the analytical propagation of uncertainty becomes impractical because of the high number of uncertain parameters.

As discussed in the "Fragility Modeling" section, the fragility and restoration parameters for each component are uncertain, and the uncertainty for each component is specified independently. Hence, the analysis here is not restricted by the type of prior distribution used for each component. Table 2 in the appendix provides the mean values of the fragility and restoration curve parameters (i.e., the lognormal distribution mean μ and standard deviation σ) for all components of the power plant. To demonstrate the uncertainty quantification techniques discussed in the previous section, $\pm 40\%$ and $\pm 30\%$ uniform uncertainty is assumed in specifying the mean and standard deviations, respectively, for each component and each damage state. These intervals were deemed reasonable for the unknown parameters based on existing expert opinion for demonstration purposes. Within these intervals, all values of the parameter are thought to be equally likely. In practice, however, each component will have an independent distribution obtained through expert judgment or empirical data.

The uncertainty in the mean downtime for a range of demand parameter values is estimated using the three approaches discussed in the previous section. The results are discussed in the following subsections. The mean downtime is estimated based on Eqs. (5) and (6) for s ranging from 0 to $2g$ in increments of $0.2g$. To build the empirical distribution $F_{\text{top}}(t|s)$, downtime (t) is considered in 2-day increments for up to 300 days. Thus, for each value of s, a mean downtime estimate is obtained for the power plant using the component fragility and restoration parameters.

Monte Carlo Simulation

A total of $N = 1{,}500$ sample sets of the 1,416 input parameters are drawn from their respective probability distributions. $N = 1{,}500$ is chosen to enable one-to-one comparison with subset simulation

Downloaded from ascelibrary.org by Clemson University on 02/26/20. Copyright ASCE. For personal use only; all rights reserved.

Table 2. Mean parameters for fragility and restoration curves of case-study power plant's components

	Fragility parameters						Restoration parameters					
	Low damage		Medium damage		High damage		Low damage		Medium damage		High damage	
Component	μ (g)	σ	μ (g)	σ	μ (g)	σ	μ (days)	σ	μ (days)	σ	μ (days)	σ
Tipper car	0.15	0.4	0.45	0.5	1.4	0.6	5	0.3	8	0.3	30	0.3
Coal silo	0.45	0.47	0.69	0.32	0.89	0.21	5	0.5	10	0.5	45	0.5
Coal pulverizer	0.25	0.5	1.2	0.7	6	0.8	5	0.3	8	0.3	30	0.3
Furnace/drum	0.45	0.47	0.69	0.32	0.89	0.21	5	0.5	10	0.5	45	0.5
Economizer	0.25	0.5	1.2	0.7	6	0.8	5	0.3	8	0.3	45	0.3
Super heater	0.25	0.5	1.2	0.7	6	0.8	5	0.3	8	0.3	30	0.3
Reheater	0.25	0.5	1.2	0.7	6	0.8	5	0.3	8	0.3	30	0.3
Steel frame support	0.25	0.5	1.4	0.6	2	0.6	7	0.3	15	0.3	60	0.3
Piping	0.25	0.35	0.4	0.35	1	0.35	5	0.3	8	0.3	30	0.3
Forced draft fan	0.25	0.5	1.2	0.7	6	0.8	5	0.3	8	0.3	30	0.3
Air recirculation fan	0.25	0.5	1.2	0.7	6	0.8	5	0.3	8	0.3	30	0.3
Air preheater	0.25	0.5	1.2	0.7	6	0.8	5	0.3	8	0.3	30	0.3
Air ducts	0.5	0.35	0.8	0.35	2	0.35	5	0.3	8	0.4	30	0.5
Feed water pump	1	0.3	1.5	0.3	2	0.3	5	0.3	8	0.3	30	0.3
Feed water storage tank	0.38	0.8	0.86	0.8	1.18	0.61	5	0.5	10	0.5	45	0.5
Deaerator tank	0.38	0.8	0.86	0.8	1.18	0.61	5	0.5	10	0.5	45	0.5
Intake pump	1	0.3	1.5	0.3	2	0.3	5	0.5	8	0.5	10	0.5
Spray dryer absorber	1.6	0.3	2	0.35	3	0.35	5	0.3	8	0.3	30	0.3
Fabric filter	1.6	0.3	2	0.35	3	0.35	5	0.3	8	0.3	30	0.3
Atomizer	1.6	0.3	2	0.35	3	0.35	5	0.3	8	0.3	30	0.3
Exhaust ducts	1.2	0.5	1.9	0.5	2	0.35	5	0.3	8	0.4	30	0.5
Electrostatic precipitator	1.6	0.3	2	0.35	3	0.35	5	0.3	8	0.3	30	0.3
Desulfurization system	0.7	0.48	1.1	0.35	1.29	0.28	5	0.5	8	0.5	45	0.5
Control room	0.8	0.3	1.2	0.3	1.5	0.3	7	0.3	10	0.3	30	0.3
Exhaust stack	0.2	0.3	0.75	0.4	1.1	0.3	10	0.3	30	0.3	60	0.3
High-pressure turbine	1.2	0.5	1.8	0.5	3.2	0.5	10	0.3	25	0.4	60	0.4
I/m-pressure turbine	1.2	0.5	1.8	0.5	3.2	0.5	10	0.3	25	0.4	60	0.4
Low-pressure turbine	1.2	0.5	1.8	0.5	3.2	0.5	10	0.3	25	0.4	60	0.4
Diesel generator	2	0.4	3.2	0.4	4	0.4	10	0.3	25	0.4	60	0.4
Generator	1	0.3	1.5	0.3	2	0.3	10	0.3	25	0.4	60	0.4
Transformer	1.2	0.6	1.5	0.6	2	0.6	8	0.2	20	0.3	45	0.3
Transmission line	1.2	0.6	1.5	0.6	2	0.6	5	0.2	8	0.3	30	0.3
Cool water pump	1	0.3	1.5	0.3	2	0.3	5	0.3	8	0.3	30	0.3
Condenser	0.5	0.3	0.8	0.3	2.5	0.3	5	0.3	8	0.3	30	0.3
Condensate pump	1	0.3	1.5	0.3	2	0.3	5	0.3	8	0.3	30	0.3
Cooling water pipeline	1.5	0.3	2	0.3	2.5	0.3	5	0.3	8	0.3	30	0.3
Intake pipe	0.5	0.3	0.8	0.3	2.5	0.3	5	0.3	8	0.3	30	0.3
Pier	0.21	0.72	0.46	0.83	0.89	1.09	10	0.3	16	0.3	75	0.3
Clam shell crane	0.29	0.3	0.45	0.3	0.67	0.3	5	0.3	8	0.3	30	0.3
Conveyor system	0.3	0.3	1.4	0.3	2	0.3	6	0.3	12	0.3	60	0.3
Siphon pipeline	0.3	0.3	0.8	0.3	2.5	0.3	5	0.2	15	0.3	45	0.3
Service water tank	0.38	0.8	0.86	0.8	1.18	0.61	5	0.5	10	0.5	45	0.5
Diesel fuel tanks	0.38	0.8	0.86	0.8	1.18	0.61	5	0.5	10	0.5	45	0.5
Emergency generator	1	0.3	1.5	0.3	2	0.3	10	0.3	25	0.4	60	0.4
Off-site power	0.3	0.3	0.6	0.3	0.8	0.3	5	1	10	1	20	1
Turbine building	0.41	0.64	0.76	0.64	1.46	0.64	7	0.8	15	0.8	60	1
Switchgear	0.7	0.3	1.4	0.3	2	0.6	5	0.2	8	0.3	30	0.3
Battery racks	1	0.3	1.5	0.3	2	0.3	5	0.2	8	0.3	30	0.3
Condensate water tank	0.38	0.8	0.86	0.8	1.18	0.61	5	0.5	10	0.5	45	0.5
Ash silo	0.38	0.8	0.86	0.8	1.18	0.61	5	0.5	10	0.5	45	0.5
Ash-handling system	0.25	0.5	0.38	0.5	0.53	0.6	5	0.3	10	0.3	30	0.3

Downloaded from ascelibrary.org by Clemson University on 02/26/20. Copyright ASCE. For personal use only; all rights reserved.

discussed in subsequent subsections, where the algorithm is set up to make 1,500 calls to the limit state function, resulting in the same computational demand. This gives 1,500 values of downtime $E(T|s)$ for PGA (s) values ranging from 0 to $2g$, plotted in Fig. 5, along with the mean curve and ± 1 standard deviation and coefficients of variation for the case-study power plant. A sufficiently large sample size is vital for prediction at the tails of the distribution. Fig. 6 shows the characterization of the tail of the cumulative distribution at $s = 1g$ with various sample sizes of N. It is observed that $N = 1{,}000$ is unable to characterize the distribution below $P = 0.001$. As seen in the figure, when a distribution with $N = 2E^5$ is assumed as a reference solution, the discrepancy in the probability estimate decreases with increasing sample size.

Subset Simulation with Modified Metropolis Algorithm

If the subset simulation consists of five intermediate levels, the use of a sample size of $N = 300$ per level results in a total of 1,500

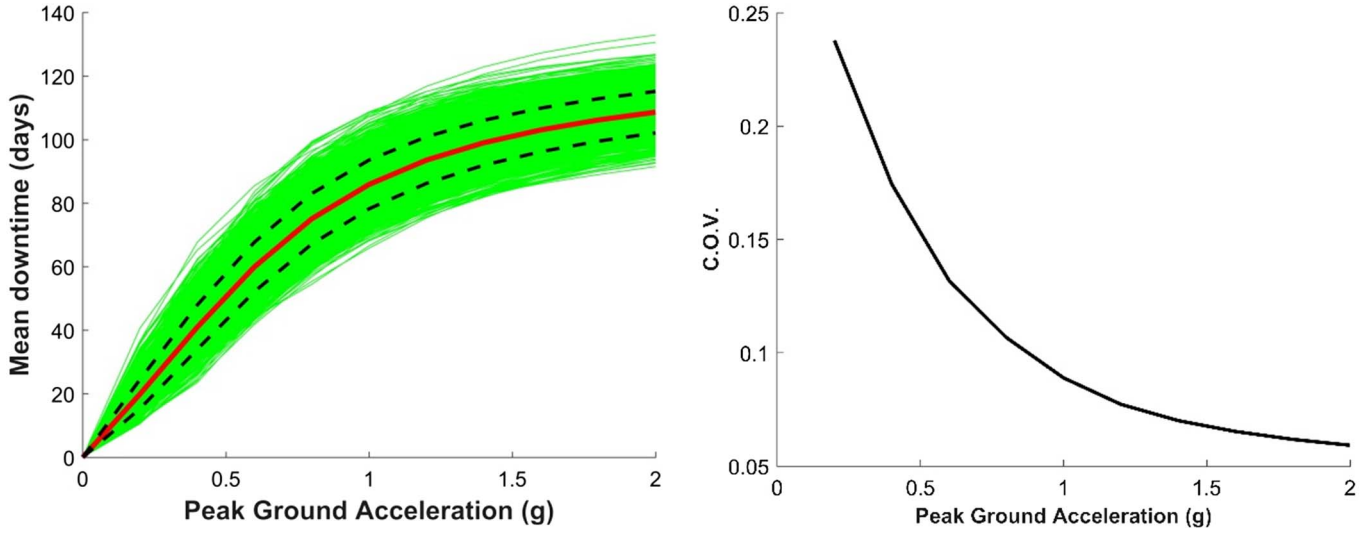

Fig. 5. Range of s (PGA in g) versus $E(T|s)$ (mean downtime in days) relations obtained for power plant via uncertainty propagation and corresponding coefficients of variation ($N = 1{,}500$).

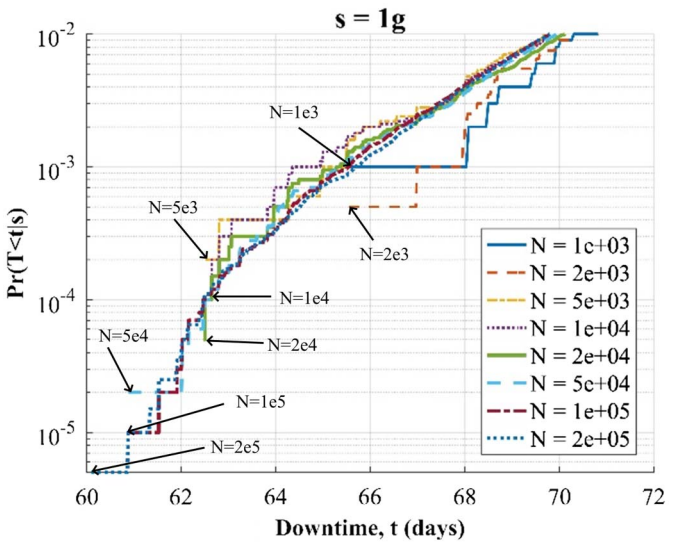

Fig. 6. Cumulative distribution of power plant's downtime corresponding to $s = 1 \times g$ estimated with different values of sample size N. The arrow heads show the end of the cumulative distribution curve.

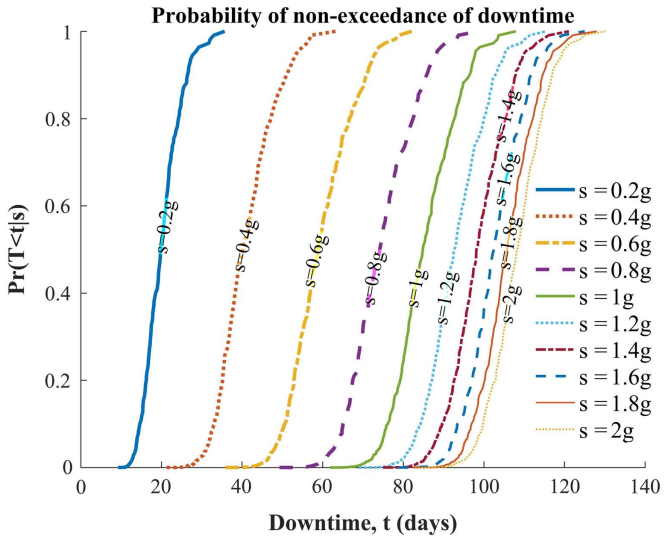

Fig. 7. Cumulative distribution functions of the power plant's downtime for demand parameter s, ranging from 0 to $2g$ obtained using subset simulation with a modified Metropolis algorithm.

samples. The failure probability p_0 at each iteration is kept constant at 0.1, and the intermediate threshold g_{t_k} is chosen accordingly. Thus, failure probability at the intermediate level m is 0.1^m. With $m = 5$, the downtime values corresponding to $P_f = 10^{-5}$ are achievable with only 1,500 samples. The resulting downtime cumulative distributions for increasing values of s are given in Fig. 7. The subset simulation estimates the power plant's threshold values of downtime d only at failure probability P_f. The intermediate threshold values corresponding to $P_f^{(i)} > P_f > P_f^{(i+1)}$ are approximated through linear interpolation. To reduce approximation errors, p_0 can be increased, although a higher number of iterations leads to additional computational cost in attaining the target failure probability. For instance, $p_0 = 0.25$ and a target probability of 10^{-5} require $m = \{[\log(10^{-5})]/[\log(0.25)]\} \approx 9$ intermediate levels, or 2,700 samples.

Subset Simulation with Multivariate Draw

In this section, the modified Metropolis algorithm is replaced by a multivariate draw to generate the candidate parameter set using the algorithm discussed in the previous section. The use of a multivariate draw results in a higher acceptance rate of samples in the failure region of the power plant. For a random walk multivariate Markov chain, a lower acceptance probability of 23.4% (Roberts et al. 1997, Carlin and Louis 2009) is typically preferred to improve efficiency in converging to the target distribution. For this study, the target distribution, which is already known to be uniform, is used as the initial distribution for the parameters. Since the initial states are distributed as the target distribution, convergence to the target distribution is immediate, and the only concern becomes sampling from the truncated part of the parameter space (i.e., it is desirable to

Downloaded from ascelibrary.org by Clemson University on 02/26/20. Copyright ASCE. For personal use only; all rights reserved.

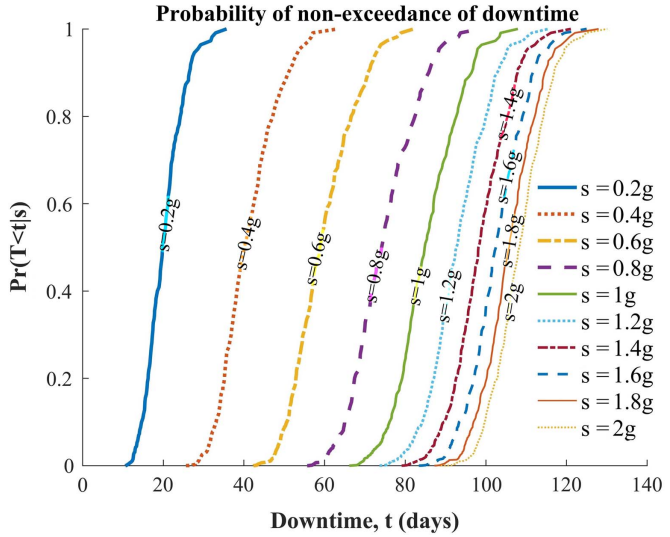

Fig. 8. Cumulative distribution functions of the power plant's downtime for demand parameter s, ranging from 0 to $2g$ obtained using subset simulation with multivariate draw.

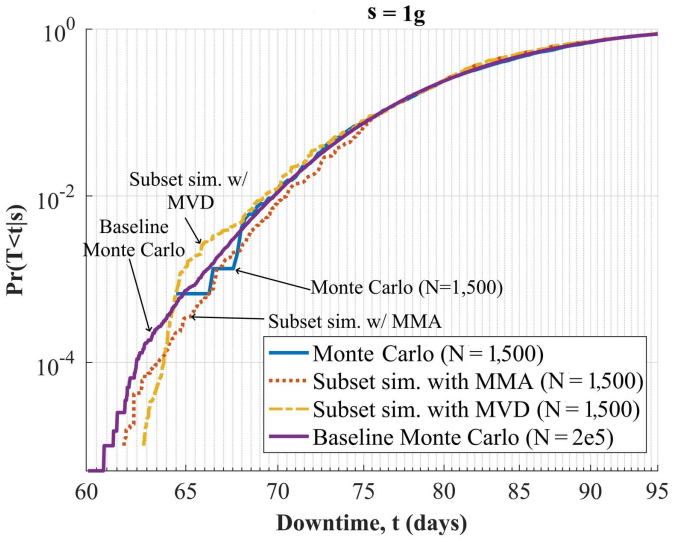

Fig. 9. Comparison of cumulative distribution functions of the power plant's downtime corresponding to $s = 1g$ with the three studied methods.

have an acceptance rate much higher than 0.234). Fig. 8 shows the cumulative distribution function of the power plant's downtime obtained using subset simulation with multivariate draw.

Fig. 9 presents the power plant's downtime distribution corresponding to $s = 1g$ obtained from Monte Carlo simulation, subset simulation using the modified Metropolis algorithm, and subset simulation using a multivariate draw. The cumulative distributions obtained using these three methods are compared with a reference solution generated using a Monte Carlo simulation with $N = 2E^5$. The advantage of using multivariate proposals over marginal proposals lies in lower computational time for the conditional sampling since the N samples are drawn collectively rather than individually; for this study's fault tree model, multivariate proposals result in three times less computational effort for the resampling algorithm using MATLAB's *mvrnd* (Matlab 2018) method. It is to be noted, however, that the majority of the computational effort in the case-study model is due to the calls to the limit state function, i.e., the fault tree model. Thus, the computational time for both algorithms remains practically equal. The primary advantage of using multivariate draw is in the increased acceptance rate: a sample acceptance rate of up to 80% was achieved using a multivariate draw, as opposed to approximately 20% with the modified Metropolis algorithm. This rate is expected to vary by system modeled. It is worth noting that the acceptance rate varies with the iteration of the subset simulation. However, the acceptance rate could be raised even higher by calibrating a scalar multiplier of the covariance matrix $\mathbf{\Sigma}_i$ for each intermediate failure region F_i during an initial burn-in period for each such region (Carlin and Louis 2009).

Conclusions

The main contribution of this paper is to provide a framework for the downtime estimation of complex industrial facilities using a system-modeling approach while considering the uncertainty in the model parameters using an efficient simulation algorithm. Relying on average estimates gives no indication of the probability of rare events that result from worst-case scenarios. Fault tree analysis allows for the consideration of the unique properties of a facility, including component layout, specific component interdependencies, system redundancies, individual component failure probabilities as functions of ground motion, beliefs about restoration time for each component, and particular damage states. Such flexibility allows for the incorporation of facility engineers' educated opinions regarding repair times and damage ratios. The input parameters of the fault tree model are the probability distribution parameters of fragility and repair times, both of which are uncertain for a variety of reasons. These uncertainties represent the degree of belief in the input parameter values that must be propagated to predict system-level downtime.

The direct Monte Carlo approach to uncertainty quantification yields accurate output distributions, but at the cost of high computational time, especially for identifying downtimes corresponding to rare occurrences (i.e., those with a very low probability). Meanwhile, a widely used rare-event simulation technique, subset simulation, provides exceptional computational efficiency in estimating the low-probability tails of downtime distribution. Subset simulation achieves target failure probability by sampling in intermediate failure regions that correspond to decreasing failure probabilities. The original subset simulation algorithm ignores the correlation between variables in intermediate failure states, resulting in suboptimal acceptance rates for the sampling. In this paper, however, it is shown that acceptance rates can be increased by replacing the original algorithm with a multivariate draw technique that leverages the sample covariance matrix. Using a multivariate draw is significantly more efficient when the parameters are highly correlated.

In this paper's case study, downtime of a coal-fired power plant was estimated for seismic hazard. The traditional Monte Carlo approach, subset simulation using a modified Metropolis algorithm, and subset simulation using multivariate draw were used to quantify the probability of the power plant exceeding a given downtime. It was found that the multivariate draw algorithm increased the acceptance rate resampling in the failure region, resulting in fewer repeated samples.

Thus, using the fault tree modeling and subset simulation with a multivariate draw algorithm allows for estimating downtime under any hazard by considering the layout of the facility, while also efficiently quantifying the uncertainty in the downtime. In the next

Downloaded from ascelibrary.org by Clemson University on 02/26/20. Copyright ASCE. For personal use only; all rights reserved.

stage of this research, the authors will focus on expanding this study's methodology to include other industrial facilities and to account for multiple possible secondary perils (e.g., a tsunami following an earthquake, as was experienced during the Fukushima tragedy).

Disclaimer

The contents of this paper represent the views of the authors alone and not those of American International Group or Clemson University.

Notation

The following symbols are used in this paper:

C = Fault tree subsystem failure event;
c = Fault tree component of a fault tree;
d = Discrete damage state of a component;
F = Failure region, or set of all $\boldsymbol{\theta}$ such that $I_F(\boldsymbol{\theta}) = 1$;
F_k = Failure region in the parameter space corresponding to the kth level in subset simulation, $(k = 1, \ldots, m)$;
$\mathcal{F}(\cdot)$ = Cumulative distribution function of the standard normal distribution;
$F_{\text{top}}(s,t)$ = Probability of system of components being unrepaired after time t, following an event of magnitude s;
$G_d(t)$ = Restoration curve; probability of the restoration time exceeding time t when a system component is in damage state d;
$g(\boldsymbol{\theta})$ = Limit state/performance function;
g^* = Threshold value for limit state function;
g^*_{target} = Rare event threshold for which failure probability is to be estimated;
$H_d(s)$ = Fragility curve; probability of exceeding damage state d given the demand parameter s;
$I_F(\boldsymbol{\theta})$ = Indicator function in failure region F (1 if system has failed i.e., $g(\boldsymbol{\theta}) < g^*_F$; 0 otherwise);
k = Level in a subset simulation;
m = Number of intermediate failure modes in subset simulation;
N = Number of samples in Monte-Carlo simulation;
N_s = Monte Carlo sample size from the Markov chain;
n = Number of uncertain parameters in a system model, i.e. number of dimensions;
n_c = Number of components in a subsystem;
n_d = Number of discrete damage states of a component;
$P(\cdot)$ = Probability of a discrete event;
p_F = Rare failure probability or probability of rare event;
$\hat{p}_F$ = Estimate of failure probability;
$q_l(\cdot\,|\theta_l^{(k)})$ = Univariate conditional proposal distribution of the parameter $\theta_l(k)$; $l = 1, \ldots, n$;
r = Acceptance ratio;
$\boldsymbol{S}_1$ = Sample covariance matrix;
s = Intensity of hazard/peril, e.g., peak ground acceleration during an earthquake;
t = Time since occurrence of hazardous event for which the system is non-functional;
$\boldsymbol{\eta} = (\eta_1, \ldots, \eta_n)$ = Logit transform of $\boldsymbol{\theta}$;
$\boldsymbol{\theta} = (\theta_1, \ldots, \theta_n)$ = Uncertain parameters of the system being modeled;
$\boldsymbol{\theta}_j^{(k)} = (\theta_1^{(k)}, \ldots, \theta_n^{(k)})_j$ = jth sample in the failure region F_k, $j = 1, \ldots, N_s$;
$\theta_l^* = (\theta_1^*, \ldots, \theta_n^*)_l$ = Candidate state, $l = 1, \ldots, n$;
ι = Nugget term;
$\mu_{d,s}$ = Median parameter of the fragility function for damage state d and earthquake intensity s;
$\mu_{d,t}$ = Median parameter of the restoration function for damage state d and time t since event;
$\pi_l(\theta_l(k))$ = Univariate marginal distribution of the parameter $\theta_l(k)$; $l = 1, \ldots, n$;
$\boldsymbol{\Sigma}$ = Covariance matrix;
$\sigma_{d,s}$ = Log standard deviation parameter of the fragility function for damage state d and earthquake intensity s;
$\sigma_{d,t}$ = Log standard deviation parameter of the restoration function for damage state d and time t since event; and
ϕ_l = Proposed value for θ_l^*.

References

Ababou, R., A. C. Bagtzoglou, and E. F. Wood. 1994. "On the condition number of covariance matrices in kriging, estimation, and simulation of random fields." *Math. Geol.* 26 (1): 99–133. https://doi.org/10.1007/BF02065878.

Alesch, D. J., and J. N. Holly. 1998. "Small business failure, survival and recovery: Lessons from the January 1994 Northridge Earthquake." In Vol. 17 of *Proc., NEHRP Conf. and Workshop on Research on the Northridge, California Earthquake of January 17th 1994*. Washington, DC: The World Bank.

Alesch, D. J., J. N. Holly, E. Mittler, and R. Nagy. 2001. *Organizations at risk: What happens when small businesses and not-for-profits encounter natural disasters*. Fairfax, VA: Public Entity Risk Institute.

ATC (Applied Technology Council). 1991. *Seismic vulnerability and impact of disruption of lifelines in the conterminous United States*. Redwood City, CA: ATC.

Au, S. K., and J. L. Beck. 2001. "Estimation of small failure probabilities in high dimensions by subset simulation." *Probab. Eng. Mech.* 16 (4): 263–277. https://doi.org/10.1016/S0266-8920(01)00019-4.

Barlyn, S. 2017. "Business interrupted: Hurricane-damaged firms dig in for insurance fight." Accessed February 17, 2019. https://www.reuters.com/article/us-storm-irma-insurance-businesses/business-interrupted-hurricane-damaged-firms-dig-in-for-insurance-fight-idUSKCN1BQ0EY.

Basoz, N. I., A. S. Kiremidjian, S. A. King, and K. H. Law. 1999. "Statistical analysis of bridge damage data from the 1994 Northridge, CA, earthquake." *Earthquake Spectra* 15 (1): 25–54. https://doi.org/10.1193/1.1586027.

Bect, J., L. Ling, and E. Vazquez. 2017. "Bayesian subset simulation." *SIAM/ASA J. Uncertainty Quantif.* 5 (1): 762–786. https://doi.org/10.1137/16M1078276.

Bradley, B. A., and R. P. Dhakal. 2008. "Error estimation of closed-form solution for annual rate of structural collapse." *Earthquake Eng. Struct. Dyn.* 37 (15): 1721–1737. https://doi.org/10.1002/eqe.833.

Brown, D. A., and S. Atamturktur. 2018. "Nonparametric functional calibration of computer models." Preprint, submitted February 19, 2016. https://arxiv.org/abs/1602.06202.

Caflisch, R. E. 1998. "Monte Carlo and quasi-Monte Carlo methods." *Acta Numer.* 7: 1–49. https://doi.org/10.1017/S0962492900002804.

Carlin, B. P., and T. A. Louis. 2009. "Approaches to statistical inferences." In *Bayesian methods for data analysis*, 3. Boca Raton, FL: CRC Press.

Carpaneto, E., G. Chicco, R. Porumb, and E. Roggero. 2005. "Probabilistic representation of the distribution system restoration times." In *Proc., CIRED 2005: 18th Int. Conf. and Exhibition on Electricity Distribution*, 1–5. London: Institution of Engineering and Technology.

Chang, S. E. 2000. "Disasters and transport systems: Loss, recovery and competition at the Port of Kobe after the 1995 earthquake." *J. Transp. Geogr.* 8 (1): 53–65. https://doi.org/10.1016/S0966-6923(99)00023-X.

Downloaded from ascelibrary.org by Clemson University on 02/26/20. Copyright ASCE. For personal use only; all rights reserved.

Downloaded from ascelibrary.org by Clemson University on 02/26/20. Copyright ASCE. For personal use only; all rights reserved.

Chang, S. E., R. T. Eguchi, and H. A. Seligson. 1996. *Estimation of the economic impact of multiple lifeline disruption: Memphis light, gas and water division case study.* Technical Rep. NCEER-96-0011. Buffalo, NY: Multidisciplinary Center for Earthquake Engineering Research.

Chang, S. E., and A. Falit-Baiamonte. 2002. "Disaster vulnerability of businesses in the 2001 Nisqually earthquake." *Global Environ. Change Part B: Environ. Hazards* 4 (2): 59–71. https://doi.org/10.1016/S1464-2867(03)00007-X.

Colombi, M., B. Borzi, H. Crowley, M. Onida, F. Meroni, and R. Pinho. 2008. "Deriving vulnerability curves using Italian earthquake damage data." *Bull. Earthquake Eng.* 6 (3): 485–504. https://doi.org/10.1007/s10518-008-9073-6.

Comerio, M. C. 2006. "Estimating downtime in loss modeling." *Earthquake Spectra* 22 (2): 349–365. https://doi.org/10.1193/1.2191017.

Der Kiureghian, A. 1996. "Structural reliability methods for seismic safety assessment: A review." *Eng. Struct.* 18 (6): 412–424. https://doi.org/10.1016/0141-0296(95)00005-4.

Ellingwood, B. R. 2001. "Earthquake risk assessment of building structures." *Reliab. Eng. Syst. Saf.* 74 (3): 251–262. https://doi.org/10.1016/S0951-8320(01)00105-3.

EPRI (Electric Power Research Institute). 2007. *Electric power research institute—Seismic experience database version 2.3*. Palo Alto, CA: EPRI.

Erdik, M., and E. Durukal. 2003. "Damage to and vulnerability of industry in the 1999 Kocaeli, Turkey, Earthquake." Chap. 19 in *Disaster risk management series No. 3: Building safer cities*, 289. Washington, DC: World Bank.

FEMA. 2010. "Hazus-MH MR5 technical manual." Accessed December 1, 2019. http://www.fema.gov/hazus.

Flammini, F., N. Mazzocca, M. Iacono, and S. Marrone. 2005. "Using repairable fault trees for the evaluation of design choices for critical repairable systems." In *Proc., 9th IEEE Int. Symp. on High-Assurance Systems Engineering (HASE '05)*, 163–172. New York: IEEE.

Gardoni, P., K. M. Mosalam, and A. der Kiureghian. 2003. "Probabilistic seismic demand models and fragility estimates for RC bridges." *J. Earthquake Eng.* 7 (spec01): 79–106. https://doi.org/10.1080/13632460309350474.

Godschalk, D. R. 2003. "Urban hazard mitigation: Creating resilient cities." *Nat. Hazard. Rev.* 4 (3): 136–143. https://doi.org/10.1061/(ASCE)1527-6988(2003)4:3(136).

Gregor, N., et al. 2014. "Comparison of NGA-West2 GMPEs." *Earthquake Spectra* 30 (3): 1179–1197. https://doi.org/10.1193/070113EQS186M.

Haario, H., E. Saksman, and J. Tamminen. 2001. "An adaptive Metropolis algorithm." *Bernoulli* 7 (2): 223–242. https://doi.org/10.2307/3318737.

Hamburger, R. O., C. Rojahn, J. Heintz, and M. Mahoney. 2012. "FEMA P58: Next-generation building seismic performance assessment methodology." In Vol. 10 of *Proc., 15th World Conf. on Earthquake Engineering*. Tokyo: International Association for Earthquake Engineering.

Hamburger, R. O., C. Rojahn, J. P. Moehle, R. Bachman, C. D. Comartin, and A. S. Whittaker. 2004. "Development of next-generation performance-based earthquake engineering design criteria for buildings." In *Proc., 13th World Conf. on Earthquake Engineering*. Tokyo: International Association for Earthquake Engineering.

Hastings, W. K. 1970. "Monte Carlo sampling methods using Markov chains and their applications." *Biometrika* 57 (1): 97–109. https://doi.org/10.1093/biomet/57.1.97.

Heatwole, N., and A. Rose. 2013. "A reduced-form rapid economic consequence estimating model: Application to property damage from US earthquakes." *Int. J. Disaster Risk Sci.* 4 (1): 20–32. https://doi.org/10.1007/s13753-013-0004-z.

Hemez, F. M., and S. Atamturktur. 2011. "The dangers of sparse sampling for the quantification of margin and uncertainty." *Reliab. Eng. Syst. Saf.* 96 (9): 1220–1231. https://doi.org/10.1016/j.ress.2011.02.015.

Higdon, D., J. Gattiker, B. Williams, and M. Rightley. 2008. "Computer model calibration using high-dimensional output." *J. Am. Stat. Assoc.* 103 (482): 570–583. https://doi.org/10.1198/016214507000000888.

Huang, Y. N., A. S. Whittaker, and N. Luco. 2011. "A probabilistic seismic risk assessment procedure for nuclear power plants: (I) Methodology." *Nucl. Eng. Des.* 241 (9): 3996–4003. https://doi.org/10.1016/j.nucengdes.2011.06.051.

Hwang, H. H., and T. Chou. 1998. "Evaluation of seismic performance of an electric substation using event tree/fault tree technique." *Probab. Eng. Mech.* 13 (2): 117–124. https://doi.org/10.1016/S0266-8920(97)00018-0.

Ibarra, L. F., and H. Krawinkler. 2005. *Global collapse of frame structures under seismic excitations*. Berkeley, CA: Pacific Earthquake Engineering Research Center.

Isumi, M., N. Nomura, and T. Shibuya. 1985. "Simulation of post-earthquake restoration of lifeline systems." *Int. J. Mass Emergencies Disasters* 3 (1): 87–105.

Karanki, D. R., H. S. Kushwaha, A. K. Verma, and S. Ajit. 2009. "Uncertainty analysis based on probability bounds (p-box) approach in probabilistic safety assessment." *Risk Anal. Int. J.* 29 (5): 662–675. https://doi.org/10.1111/j.1539-6924.2009.01221.x.

Kim, S. H., and M. Q. Feng. 2003. "Fragility analysis of bridges under ground motion with spatial variation." *Int. J. Non Linear Mech.* 38 (5): 705–721. https://doi.org/10.1016/S0020-7462(01)00128-7.

Kircher, C. A., R. V. Whitman, and W. T. Holmes. 2006. "Hazus earthquake loss estimation methods." *Nat. Hazard. Rev.* 7 (2): 45–59. https://doi.org/10.1061/(ASCE)1527-6988(2006)7:2(45).

Kiremidjian, A. S., K. Ortiz, R. Nielsen, and B. Safavi. 1985. *Seismic risk to major industrial facilities*. Report to the National Science Foundation, Grant No. CEE-8116997 and Grant No. CEE-8400479, January. Stanford, CA: Dept. of Civil and Environmental Engineering, Stanford Univ.

Kozin, F., and H. Zhou. 1990. "System study of urban response and reconstruction due to earthquake." *J. Eng. Mech.* 116 (9): 1959–1972. https://doi.org/10.1061/(ASCE)0733-9399(1990)116:9(1959).

Krausmann, E., and A. M. Cruz. 2013. "Impact of the 11 March 2011, Great East Japan earthquake and tsunami on the chemical industry." *Nat. Hazard.* 67 (2): 811–828. https://doi.org/10.1007/s11069-013-0607-0.

Kunz, M., et al. 2013. "Investigation of superstorm Sandy 2012 in a multi-disciplinary approach." *Nat. Hazards Earth Syst. Sci.* 13 (10): 2579–2598. https://doi.org/10.5194/nhess-13-2579-2013.

Lallemant, D., A. Kiremidjian, and H. Burton. 2015. "Statistical procedures for developing earthquake damage fragility curves." *Earthquake Eng. Struct. Dyn.* 44 (9): 1373–1389. https://doi.org/10.1002/eqe.2522.

Lantada, N., J. Irizarry, A. H. Barbat, X. Goula, A. Roca, T. Susagna, and L. G. Pujades. 2010. "Seismic hazard and risk scenarios for Barcelona, Spain, using the Risk-UE vulnerability index method." *Bull. Earthquake Eng.* 8 (2): 201–229. https://doi.org/10.1007/s10518-009-9148-z.

Lapp, S. A., and G. J. Powers. 1977. "Computer-aided synthesis of fault-trees." *IEEE Trans. Reliab.* 26 (1): 2–13. https://doi.org/10.1109/TR.1977.5215060.

Lee, W. S., D. L. Grosh, F. A. Tillman, and C. H. Lie. 1985. "Fault tree analysis, methods, and applications: A review." *IEEE Trans. Reliab.* 34 (3): 194–203. https://doi.org/10.1109/TR.1985.5222114.

Lindhe, A., L. Rosén, T. Norberg, and O. Bergstedt. 2009. "Fault tree analysis for integrated and probabilistic risk analysis of drinking water systems." *Water Res.* 43 (6): 1641–1653. https://doi.org/10.1109/TPWRS.2007.907587.

Liu, H., R. A. Davidson, and T. V. Apanasovich. 2007. "Statistical forecasting of electric power restoration times in hurricanes and ice storms." *IEEE Trans. Power Syst.* 22 (4): 2270–2279. https://doi.org/10.1109/TPWRS.2007.907587.

Liu, J. S., W. H. Wong, and A. Kong. 1994. "Covariance structure of the Gibbs sampler with applications to the comparisons of estimators and augmentation schemes." *Biometrika* 81 (1): 27–40. https://doi.org/10.1093/biomet/81.1.27.

Logothetis, D., and K. Trivedi. 1997. "The effect of detection and restoration times for error recovery in communication networks." *J. Network Syst. Manage.* 5 (2): 173–195. https://doi.org/10.1023/A:1018722928191.

Lopez, O. A., A. K. Chopra, and J. J. Hernandez. 2000. "Critical response of structures to multicomponent earthquake excitation." *Earthquake Eng. Struct. Dyn.* 29 (12): 1759–1778. https://doi.org/10.1002/1096-9845(200012)29:12<1759::AID-EQE984>3.0.CO;2-K.

Lou, L., and A. Zerva. 2005. "Effects of spatially variable ground motions on the seismic response of a skewed, multi-span, RC highway bridge." *Soil Dyn. Earthquake Eng.* 25 (7): 729–740. https://doi.org/10.1016/j.soildyn.2004.11.016.

Lupoi, A., P. Franchin, P. E. Pinto, and G. Monti. 2005. "Seismic design of bridges accounting for spatial variability of ground motion." *Earthquake Eng. Struct. Dyn.* 34 (4–5): 327–348. https://doi.org/10.1002/eqe.444.

Matlab. 2018. "Mvrnd: Multivariate normal random numbers." Accessed February 2, 2019. https://www.mathworks.com/help/stats/mvnrnd.html.

Metropolis, N., A. W. Rosenbluth, M. N. Rosenbluth, A. H. Teller, and E. Teller. 1953. "Equation of state calculations by fast computing machines." *J. Chem. Phys.* 21 (6): 1087–1092. https://doi.org/10.1063/1.1699114.

Nateghi, R., S. D. Guikema, and S. M. Quiring. 2011. "Comparison and validation of statistical methods for predicting power outage durations in the event of hurricanes." *Risk Anal.* 31 (12): 1897–1906. https://doi.org/10.1111/j.1539-6924.2011.01618.x.

Noh, H. Y., D. Lallemant, and A. S. Kiremidjian. 2015. "Development of empirical and analytical fragility functions using kernel smoothing methods." *Earthquake Eng. Struct. Dyn.* 44 (8): 1163–1180. https://doi.org/10.1002/eqe.2505.

Norberg, T., L. Rosén, and A. Lindhe. 2009. "Added value in fault tree analyses." In *Proc., 2008 'Safety, Reliability and Risk Analysis: Theory, Methods and Applications', Joint ESREL (European Safety and Reliability) and SRA-Europe (Society for Risk Analysis Europe) Conf.*, 1041–1049. London: Taylor & Francis.

Pagni, C. A., and L. N. Lowes. 2006. "Fragility functions for older reinforced concrete beam-column joints." *Earthquake Spectra* 22 (1): 215–238. https://doi.org/10.1193/1.2163365.

Pinto, P. E., R. Giannini, and P. Franchin. 2004. *Seismic reliability analysis of structures*. Pavia, Italy: IUSS Press.

Porter, K. 2015. "Beginner's guide to fragility, vulnerability, and risk." In *Encyclopedia of earthquake engineering*, 235–260. New York: Springer.

Porter, K., and K. Ramer. 2012. "Estimating earthquake-induced failure probability and downtime of critical facilities." *J. Bus. Continuity Emergency Plann.* 5 (4): 352–364.

Rao, K. D., V. Gopika, V. S. Rao, H. S. Kushwaha, A. K. Verma, and A. Srividya. 2009. "Dynamic fault tree analysis using Monte Carlo simulation in probabilistic safety assessment." *Reliab. Eng. Syst. Saf.* 94 (4): 872–883. https://doi.org/10.1016/j.ress.2008.09.007.

Robert, C., and G. Casella. 2013. *Monte Carlo statistical methods*. New York: Springer.

Roberts, G. O., A. Gelman, and W. R. Gilks. 1997. "Weak convergence and optimal scaling of random walk Metropolis algorithms." *Ann. Appl. Probab.* 7 (1): 110–120. https://doi.org/10.1214/aoap/1034625254.

Roberts, N. H., W. E. Vesely, D. F. Haasl, and F. F. Goldberg. 1981. *Fault tree handbook NUREG-0492*. Washington, DC: US Government Printing Office.

Rossetto, T., and A. Elnashai. 2005. "A new analytical procedure for the derivation of displacement-based vulnerability curves for populations of RC structures." *Eng. Struct.* 27 (3): 397–409. https://doi.org/10.1016/j.engstruct.2004.11.002.

Ruijters, E., and M. Stoelinga. 2015. "Fault tree analysis: A survey of the state-of-the-art in modeling, analysis and tools." *Comput. Sci. Rev.* 15 (Feb): 29–62. https://doi.org/10.1016/j.cosrev.2015.03.001.

Sabetta, F., A. Goretti, and A. Lucantoni. 1998. "Empirical fragility curves from damage surveys and estimated strong ground motion." In *Proc., 11th European Conf. on Earthquake Engineering*. Rotterdam, Netherlands: A.A. Balkema.

Shinozuka, M., M. Q. Feng, H. K. Kim, and S. H. Kim. 2000. "Nonlinear static procedure for fragility curve development." *J. Eng. Mech.* 126 (12): 1287–1295. https://doi.org/10.1061/(ASCE)0733-9399(2000)126:12(1287).

Shinozuka, M., A. Rose, and R. T. Eguchi. 1998. *Engineering and socioeconomic impacts of earthquakes: An analysis of electricity lifeline disruptions in the New Madrid area*. Monograph No. 2. Buffalo, NY: Multidisciplinary Center for Earthquake Engineering Research.

Shome, N. 1999. "Probabilistic seismic demand analysis of nonlinear structures." Ph.D. dissertation, Dept. of Civil and Environmental Engineering, Stanford Univ.

Simpson, D. M., T. D. Rockaway, T. A. Weigel, P. A. Coomes, and C. O. Holloman. 2005. "Framing a new approach to critical infrastructure modelling and extreme events." *Int. J. Crit. Infrastruct.* 1 (2–3): 125–143. https://doi.org/10.1504/IJCIS.2005.006115.

Singhal, A., and A. S. Kiremidjian. 1996. "Method for probabilistic evaluation of seismic structural damage." *J. Struct. Eng.* 122 (12): 1459–1467. https://doi.org/10.1061/(ASCE)0733-9445(1996)122:12(1459).

Tatano, H., and Y. Kajitani. 2012. "Production capacity losses due to the 311 disaster—Facility damage and lifeline disruption impacts." In *Proc., Int. Disaster and Risk Conf.*, 26–30. Davos, Switzerland: Global Risk Forum GRF Davos.

Tate, E., C. Muñoz, and J. Suchan. 2015. "Uncertainty and sensitivity analysis of the HAZUS-MH flood model." *Nat. Hazard. Rev.* 16 (3): 04014030. https://doi.org/10.1061/(ASCE)NH.1527-6996.0000167.

Tierney, K. J. 1997. "Business impacts of the Northridge earthquake." *J. Contingencies Crisis Manage.* 5 (2): 87–97. https://doi.org/10.1111/1468-5973.00040.

Tierney, L., and A. Mira. 1999. "Some adaptive Monte Carlo methods for Bayesian inference." *Stat. Med.* 18 (17–18): 2507–2515. https://doi.org/10.1002/(SICI)1097-0258(19990915/30)18:17/18<2507::AID-SIM272>3.0.CO;2-J.

Unanwa, C. O., J. R. McDonald, K. C. Mehta, and D. A. Smith. 2000. "The development of wind damage bands for buildings." *J. Wind Eng. Ind. Aerodyn.* 84 (1): 119–149. https://doi.org/10.1016/S0167-6105(99)00047-1.

US Nuclear Regulatory Commission. 1983. *PRA procedures guide NUREG/CR-2300*. Washington, DC: US Nuclear Regulatory Commission.

Vesely, W. E., F. F. Goldberg, N. H. Roberts, and D. F. Haasl. 1981. *Fault tree handbook (No. NUREG-0492)*. Washington, DC: Nuclear Regulatory Commission.

Wald, D. J., V. Quitoriano, T. H. Heaton, and H. Kanamori. 1999. "Relationships between peak ground acceleration, peak ground velocity, and modified Mercalli intensity in California." *Earthquake Spectra* 15 (3): 557–564. https://doi.org/10.1193/1.1586058.

Webb, G. R., K. J. Tierney, and J. M. Dahlhamer. 2000. "Businesses and disasters: Empirical patterns and unanswered questions." *Nat. Hazard. Rev.* 1 (2): 83–90. https://doi.org/10.1061/(ASCE)1527-6988(2000)1:2(83).

Williams, B., D. Higdon, J. Gattiker, L. Moore, M. McKay, and S. Keller-McNulty. 2006. "Combining experimental data and computer simulations, with an application to flyer plate experiments." *Bayesian Anal.* 1 (4): 765–792. https://doi.org/10.1214/06-BA125.

Yang, L., Y. Kajitani, H. Tatano, and X. Jiang. 2016. "A methodology for estimating business interruption loss caused by flood disasters: Insights from business surveys after Tokai Heavy Rain in Japan." *Nat. Hazard.* 84 (1): 411–430. https://doi.org/10.1007/s11069-016-2534-3.

Zhang, R. H. 1992. "Lifeline interaction and post-earthquake urban system reconstruction." In Vol. 5 of *Proc., 10th WCEE*, 475. Rotterdam, Netherlands: A.A. Balkema.

Zhang, Y. H., Q. S. Li, J. H. Lin, and F. W. Williams. 2009. "Random vibration analysis of long-span structures subjected to spatially varying ground motions." *Soil Dyn. Earthquake Eng.* 29 (4): 620–629. https://doi.org/10.1016/j.soildyn.2008.06.007.

Zuev, K. M., J. L. Beck, S. K. Au, and L. S. Katafygiotis. 2012. "Bayesian post-processor and other enhancements of Subset Simulation for estimating failure probabilities in high dimensions." *Comput. Struct.* 92 (Feb): 283–296. https://doi.org/10.1016/j.compstruc.2011.10.017.

Zuev, K. M., and L. S. Katafygiotis. 2011. "Modified Metropolis–Hastings algorithm with delayed rejection." *Probab. Eng. Mech.* 26 (3): 405–412. https://doi.org/10.1016/j.probengmech.2010.11.008.

Downloaded from ascelibrary.org by Clemson University on 02/26/20. Copyright ASCE. For personal use only; all rights reserved.